

Contrasting the effect of aerosol properties on the planetary boundary layer height in Beijing and Nanjing

Xin Huang^{a,1}, Yuying Wang^{a,*}, Yi Shang^a, Xiaorui Song^a, Rui Zhang^a, Yuxiang Wang^a, Zhanqing Li^b, Yuanjian Yang^a

^a Key Laboratory for Aerosol–Cloud Precipitation of China Meteorological Administration/Special Test Field of National Integrated Meteorological Observation, Nanjing University of Information Science Technology, Nanjing, 210044, China

^b Earth System Science Interdisciplinary Center, Department of Atmospheric and Oceanic Science, University of Maryland, College Park, MD, 20740, USA

HIGHLIGHTS

- The evolution of planetary boundary layer heights (PBLHs) in Nanjing and Beijing differ.
- The PBLH is more sensitive to the variation in PM_{2.5} mass concentration in Nanjing than in Beijing.
- Aerosol type makes a difference in aerosol–PBL interactions in Nanjing and Beijing.

ABSTRACT

The evolution of the planetary boundary layer (PBL) and the effect of aerosols on the PBL in Beijing and Nanjing were compared based on measurements made during two long-term field campaigns. Monthly PBL height (PBLH) trends in Nanjing and Beijing were similar, opposite to those of the mass concentration of particles with diameters less than 2.5 μm (PM_{2.5}). This phenomenon was more obvious in Nanjing than in Beijing. The negative correlation between PBLH and PM_{2.5} mass concentration was weaker in Nanjing than in Beijing. The PBLH varied during the day. Heavy aerosol pollution made this variation weak in autumn and winter in Beijing. Further results suggest that out of all the seasons, summertime PM_{2.5} had the greatest influence on the evolution of the PBL. The PBLH was more sensitive to the variation in PM_{2.5} mass concentration in Nanjing than in Beijing. Aerosol type (scattering or absorbing) had a weak effect on the evolution of the PBLH in Nanjing, but absorbing aerosols played a dominant role in Beijing. Our results highlight the cross-regional difference in aerosol–PBL interactions.

1. Introduction

The planetary boundary layer (PBL) is the atmospheric layer closest to the Earth's surface. Meteorological conditions in the PBL have a direct impact on human activities (Garratt, 1994). The PBL is a key layer for the interaction of various systems of the Earth (Stull, 1988). The vertical transport of heat, momentum, and water vapor is driven by turbulent processes in the PBL, leading to strong diurnal variations of meteorological variables near the surface. The PBL height (PBLH) is about 1–1.5 km. The PBLH is a key parameter indicating turbulent mixing, air up-draft, convective cloud initiation and development, atmospheric pollutant diffusion, and atmospheric environmental capacity (Therry and Lacarrère, 1983; Hong and Pan, 1996; Beyrich, 1997; Collier et al., 2005; Qu et al., 2017). Multi-scale processes in the PBL are thus important in many models, including mesoscale meteorological models, atmospheric circulation models, numerical weather prediction models,

global climate models, and air quality models. The PBLH is affected by many factors, such as wind speed, clouds, surface temperature, and surface humidity. On the one hand, these factors, e.g., clouds, play an important role in changing the amount of solar radiation reaching the ground, which is closely related to the temporal variation of the PBLH (Tie et al., 2007). On the other hand, factors such as wind speed affect turbulence (Guinot et al., 2006), further affecting the evolution of the PBL (Wei et al., 2017).

Aerosols affect the PBLH by influencing the transfer of solar radiation (Kan et al., 2008; Deng et al., 2010; Park et al., 2016; Li et al., 2017). According to their optical properties, aerosols can be divided into scattering and absorbing aerosols. Scattering aerosols scatter solar radiation, leading to negative radiative forcing that cools the ground and the atmosphere. Absorbing aerosols absorb solar radiation, producing positive radiative forcing, which heats the atmosphere (Yu et al., 2002; Jacobson and Kaufman, 2006; Jacobson et al., 2007; Zhang et al., 2010;

* Corresponding author.

E-mail address: yuyingwang@nuist.edu.cn (Y. Wang).

¹ The authors contributed equally.

Forkel et al., 2011; Péré et al., 2011; Miao et al., 2017; Qu et al., 2017; Song et al., 2021). The interaction between aerosols and the PBL mainly manifests as aerosols inhibiting sensible and latent heat surface fluxes. This disturbance of the ground energy balance and atmospheric radiation by aerosols causes changes in meteorological parameters, affecting the structure and development of the PBL (Yu et al., 2002; Jacobson and Kaufman, 2006; Jacobson et al., 2007; Péré et al., 2011; Su et al., 2020). This, in turn, affects aerosol concentrations and their distributions within the PBL (Forkel et al., 2011; Zhang et al., 2010).

Many studies have investigated aerosol-PBL interactions in China, as reviewed by Li et al. (2016, 2017), concluding that absorbing aerosols not only alter atmospheric thermodynamics and stability but also push down the PBLH. Miao et al. (2017) used multi-source data to study the relationship between near-surface particulate matter (PM) and the summertime PBLH near Beijing, finding that synoptic patterns have an important impact on aerosol-PBL interactions. Pan et al. (2019) found that there was a negative nonlinear correlation between the PBLH and the mass concentration of PM with diameters less than 2.5 μm (PM_{2.5}) in Shanghai. When the PBLH was less than 400 m, the change in PM_{2.5} tended to be extremely sensitive to the change in PBLH. In addition, correlations between the PM_{2.5} mass concentration and the PBLH were higher in spring and winter than in other seasons. Song et al. (2021) reported that there was also a significant negative correlation between the PBLH and PM_{2.5} mass concentration in Guangzhou. In Nanjing, Qu et al. (2017) suggested that there was a strong correlation between the PBLH and PM, especially under heavy aerosol pollution conditions. A low PBLH often occurs under conditions of low wind speed and high relative humidity, leading to a high PM_{2.5} mass concentration and low visibility, enhancing the stability of the PBLH.

The effect of absorbing aerosols on the evolution of the PBL has recently attracted much attention. Yu et al. (2002) and Pandithurai et al. (2008) used the one-dimensional Coupled Atmosphere-Plant Soil model to investigate the effect of absorbing aerosols on the evolution of the PBL. They found that absorbing aerosols can heat the atmosphere in the PBL, reducing the amount of solar radiation reaching the ground and reducing the water vapor content in the PBL. In the Pearl River Delta region, Wendisch et al. (2008) discussed the effect of absorbing aerosol radiative forcing on the PBL, showing that downwelling solar fluxes at the surface decreased by 160 W m⁻² and that the maximum heating rate at the top of the aerosol layer was 7–8 K d⁻¹. Absorbing aerosol radiative forcing led to the generation of a more stable PBL structure, lowering the PBLH. Ding et al. (2016) demonstrated that absorbing aerosols induced heating in the PBL, particularly in the upper PBL, and that the resulting decreased surface heat fluxes substantially suppressed the development of the PBL.

In summary, previous studies have investigated aerosol-PBL interactions at different locations in China. Lee et al. (2007) noted that the amounts of scattering and absorbing aerosols are diverse across China. More studies differentiating the effects of scattering and absorbing aerosols on the evolution of the PBL are needed. For these reasons, this study compares aerosol-PBL interactions in two megacities, i.e., Beijing and Nanjing, located in the North China Plain and the Yangtze River Delta, respectively. The goal is to acquire a deeper understanding of the effect of aerosol properties on the evolution of the PBL.

This paper is structured as follows. Section 2 presents details about the experiments and methodology. Section 3 discusses and analyzes the monthly and seasonal variations of PBLH and PM_{2.5} mass concentration and the effect of aerosols on the evolution of the PBL. Major conclusions are summarized in section 4.

2. Experiments and methodology

2.1. Observation sites and field campaigns

Measurements made in Nanjing and Beijing (Fig. S1) are used in this study. A long-term comprehensive field experiment lasting for more

than two years (from August 2017 to October 2019) was conducted at a suburban site in Beijing (39.81°N, 116.48°E), followed by a one-year campaign from August 2020 to December 2021 in Nanjing (32.18°N, 118.72°E), during which aerosol properties and the PBL were measured and derived, respectively.

The Beijing site is located along the south of the 5th beltway, at the Beijing Meteorological Observatory which serves as a baseline station providing many routine meteorological measurements to the China Meteorological Administration. These routine measurements are supplemented with measurements conducted to test new instruments. It is surrounded by the Fifth Ring Road (semi-highway), industrial parks, and residential communities. Aerosol sources in this area are mainly from anthropogenic emissions. Wang et al. (2021) provided more information about this site.

The Nanjing site is located on the campus of the Nanjing University of Information Science and Technology. Nanjing is one of the central cities in the Yangtze River Delta, with a population of 9.3 million. Influenced by the monsoon system in East Asia, the prevailing wind direction in Nanjing changes greatly between different seasons. North-east winds dominate in winter, and east and southeast winds dominate in summer. Aerosol sources in this region vary and include industrial emissions, traffic emissions, biomass burning, and the transmission of dust aerosols from northwestern China. The aerosol composition is thus complex in Nanjing.

2.2. Instrumentation

The instruments used in the experiments included a micro-pulse lidar (MPL; Sigma Space Corp.), an Aerodyne aerosol chemical speciation monitor (ACSM), and a seven-wavelength aethalometer (AE-33, Magee Scientific Corporation).

The MPL pulse repetition rate was 2.5 kHz at the 532-nm wavelength. The vertical resolution of backscatter profiles was 15 m, and the temporal resolution was 10 s. Due to the incomplete laser pulse, there was a 150-m blind zone near the surface. As a standard procedure, background subtraction, saturation, overlap, post pulse, and range correction were applied to raw MPL data to derive the normalized signal (Campbell et al., 2002, 2003).

The ACSM was equipped with a PM_{2.5} lens system, capture vaporizer, and quadrupole mass spectrometer measuring the mass concentrations of non-refractory aerosol chemical species in PM_{2.5}, including organics (Org), nitrate (NO₃⁻), sulfate (SO₄²⁻), ammonium (NH₄⁺), and chloride (Cl⁻) (Peck et al., 2016; Xu et al., 2017; Zhang et al., 2017; Wang et al., 2021). The mass concentration of black carbon (BC) aerosols was measured by the AE-33 aethalometer. In this study, aerosol chemical compositions detected by the ACSM were identified as scattering aerosols, while BC detected by the AE-33 aethalometer were identified as absorbing aerosols. The PM_{2.5} mass concentration was obtained by adding the mass concentrations of the two types of aerosols.

2.3. Calculating the PBLH

Based on atmospheric optical characteristics, the PBLH is usually determined as the height at which the negative gradient of the backscatter coefficient detected by the ground-based MPL first appears (Boers and Eloranta, 1986). This is because there is always a large gradient of aerosols between the boundary layer and the free troposphere. Therefore, the PBLH is considered to be the midpoint of the entrainment zone. The measurements have been widely used (Liu et al., 2016; Pan et al., 2019) and we used this measurement to calculate the PBLH in the daytime [from 08:00 Beijing Time (BJT) to 18:00 BJT].

According to the algorithm proposed by He et al. (2006), the original signal obtained by the MPL is

$$p(z) = \frac{Q_c(z)CE\beta(z)T^2}{z^2} + n_b(z) + n_{ap}(z) \quad (1)$$

$$DTC[P(z)]$$

where $p(z)$ is the measured signal return in photoelectron counts per second at range z , $T^2 = \exp(-2 \int_0^z \sigma(r) dr)$ is the atmospheric transmission, $\sigma(r)$ is the extinction coefficient of the laser source to the target, $Q_c(z)$ is the overlap correction factor in the transceiver system, C is the dimensional system calibration constant, E is the transmitted laser pulse energy, $\beta(z)$ is the backscatter cross-receiver system, n_b is the background contribution from ambient light, n_{ap} is the pulse correction after the run of the detector, and DTC is the detector offset dead-time correction. After the above correction, the normalized relative backscatter (NRB) signal can be obtained, calculated after correction as

$$NRB(z) = \{p(z) \times DTC[P(z)] - n_b(z) - n_{ap}(z)\} \times z^2 \quad (2)$$

The vertical profile of $NRB(z)$ reflects the vertical profile of atmospheric aerosols. The normalized lidar range-corrected signal (RCS) gradient (NSG) is defined as

$$NSG(z) = \frac{\Delta NRB(z)}{\Delta z \times NRB(z)} \quad (3)$$

where Δz is the lidar vertical resolution. With this algorithm, the PBLH is determined as the altitude where the normalized RCS gradient reaches a minimum (Pan et al., 2019).

To reflect the impact of aerosols on the PBLH accurately, data during precipitation periods were excluded from the analysis.

3. Results and discussion

3.1. Monthly and seasonal variations of PBLH and $PM_{2.5}$ mass concentration in Nanjing and Beijing

Fig. 1 shows monthly variations of PBLH and $PM_{2.5}$ mass concentration in the daytime in Nanjing and Beijing. PBLHs in Nanjing and Beijing had similar monthly trends (Fig. 1a). PBLHs in summer and autumn months were higher than in winter and spring months, with the PBLH reaching its maximum value in July. Due to differences in observation period and region, the PBLH over the two sites differed. The PBLH over Beijing was significantly lower than that over Nanjing for all months. The average PBLH over Nanjing was about 200 m higher than that over Beijing. PBLH differences between Nanjing and Beijing were relatively small in winter.

Monthly variations in $PM_{2.5}$ mass concentration in Nanjing and Beijing (Fig. 1b) show that the $PM_{2.5}$ mass concentration in Beijing was always higher than that in Nanjing except in September. The monthly mean $PM_{2.5}$ mass concentration in Beijing peaked at $66.48 \mu\text{g}/\text{m}^3$ in November, attributed to three heavy pollution processes that occurred then (Fig. S2). Comparing the monthly variations of PBLH and $PM_{2.5}$ mass concentration, the opposite PBLH and $PM_{2.5}$ mass concentration trends in Nanjing are more clearly seen than in Beijing. In July, the $PM_{2.5}$ mass concentration in Nanjing was at its lowest, and the PBLH was at its highest. This is because the high PBLH can enhance the vertical dispersion of $PM_{2.5}$. This inverse correlation between PBLH and $PM_{2.5}$ is consistent with previously reported results (Qu et al., 2017; Lou et al., 2019).

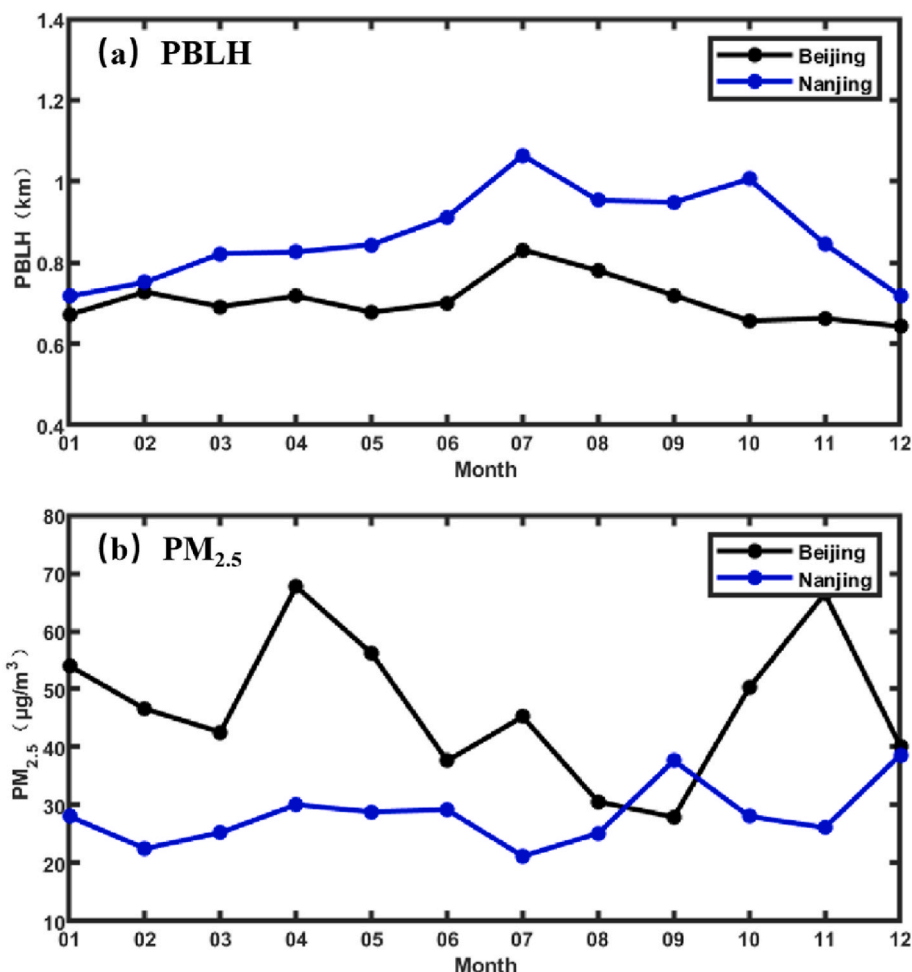


Fig. 1. Monthly variations of (a) PBLH and (b) $PM_{2.5}$ mass concentration in Beijing (black lines) and Nanjing (blue lines).

Fig. 2 shows seasonal variations in PBLH at the two sites. The mean PBLH and its variability in summer in Nanjing (0.35–1.49 km, with a median value of 0.97 km) were higher than those in other seasons. In winter, the mean PBLH was at its lowest (0.29–1.16 km, with a median value of 0.73 km). The PBLH in autumn was slightly lower than in summer, with a median value of 0.94 km. The PBLH in spring was 0.27–1.40 km, with a median value of 0.82 km.

The PBLH and its variability in summer in Beijing were also at their highest (0.33–1.17 km, with a median value of 0.73 km) in all seasons. The high PBLH in summer is likely related to the high temperature in summer. High temperatures are conducive to the development of the PBL (Stull, 1988). The highly variable PBLH in summer is likely caused by the various synoptic patterns in this season. PBLHs in spring, autumn, and winter are similar in Nanjing, with median values of 0.71 km, 0.70 km, and 0.70 km, respectively. During these three seasons, more than 90% of PBLH values were between 0.34 and 0.99 km. At both sites, the $PM_{2.5}$ mass concentration was lowest in summer and highest in winter (Fig. S3). Overall, the seasonal trend of PBLH was opposite to that of $PM_{2.5}$ mass concentration.

3.2. Effect of aerosol pollution on the evolution of the PBL

Fig. 3 shows the daytime variations of PBLH and $PM_{2.5}$ mass concentration at the two sites in different seasons. $PM_{2.5}$ mass concentrations clearly varied during the day in Nanjing and Beijing, especially in Nanjing. However, daytime variations of the PBLH in autumn and winter in Beijing were relatively small. The sharp increase in $PM_{2.5}$ mass concentration in autumn and winter in Beijing may be one of the reasons for the inhibition of the development of the PBL over Beijing.

Fig. 3 also shows that the daytime variations of $PM_{2.5}$ mass concentration in different seasons differed between Beijing and Nanjing. In Nanjing, minimum values appeared at ~16:00 BJT. In Beijing, minimum values appeared in the afternoon (also at ~16:00 BJT) in spring and summer, while they appeared in the morning (at ~10:00 BJT) in autumn and winter. In addition, $PM_{2.5}$ mass concentrations always decreased with the lifting of the PBL in the daytime. Figs. S4 and S5 further show that the PBLH and the $PM_{2.5}$ mass concentration are negatively correlated in all seasons at the two sites. The influence of $PM_{2.5}$ mass concentration on the development of the PBL is similar in different seasons but to different degrees.

To study the effect of aerosol pollution levels on the PBLH, days are divided into four groups according to the daily mean $PM_{2.5}$ mass concentration: clean days ($PM_{2.5} \leq 35 \mu\text{g}/\text{m}^3$), mildly polluted days ($35 \mu\text{g}/\text{m}^3 < PM_{2.5} \leq 75 \mu\text{g}/\text{m}^3$), moderately polluted days ($75 \mu\text{g}/\text{m}^3 < PM_{2.5} \leq 115 \mu\text{g}/\text{m}^3$), and heavily polluted days ($PM_{2.5} \geq 115 \mu\text{g}/\text{m}^3$). Fig. 4 shows daytime variations of the PBLH for these four groups in Nanjing and Beijing. The PBLH decreased significantly with increasing levels of aerosol pollution at the two sites, indicating that the $PM_{2.5}$ mass concentration affects the PBLH. This decrease in PBLH as the pollution level

increased was greater in Nanjing than in Beijing. On moderately and heavily polluted days, the PBLH weakly varied at the two sites, illustrating that other factors (such as solar radiation) have little influence on the evolution of the PBL when $PM_{2.5}$ mass concentrations are high. Fig. 4a also suggests that there was a large change in the PBLH from mildly polluted days to moderately polluted days in Nanjing.

Compared with more polluted days, the development of the PBL is more clearly seen on clean days. This also indicates that an increase in $PM_{2.5}$ can inhibit the development of the PBL. For example, in Nanjing, the daytime PBLH on moderately polluted days only reached 400–500 m, while the PBLH on clean days reached 800–1000 m (Fig. 4a). Also, the maximum value of the PBLH appeared at 14:30 BJT on clean days, half an hour earlier than on moderately polluted days. This is likely because the lower amount of solar radiation reaching the ground and weak atmospheric turbulence is not beneficial to the development of the PBL under high aerosol pollution conditions.

Density diagrams of the relationships between PBLH and $PM_{2.5}$ mass concentration and their fitted curves for the two sites show negative correlations, both with low coefficients of determination (Fig. 5). This is because other factors, such as turbulence, temperature and humidity, weather patterns, and atmospheric stability, also affect the PBLH (Tie et al., 2007; Freire and Dias, 2013; Blay-Carreras et al., 2014; Reen et al., 2014). The correlation between the PBLH and $PM_{2.5}$ mass concentration was stronger in Beijing than in Nanjing.

Fig. 5 also shows that the correlation between PBLH and $PM_{2.5}$ weakened as the $PM_{2.5}$ mass concentration increased, consistent with the results shown in Fig. 4. In this study, the ratio of PBLH to $PM_{2.5}$ mass concentration (PBLH/ $PM_{2.5}$, unit: $\text{m}^4/\mu\text{g}$) is proposed to quantify the effect of aerosol pollution on the evolution of the PBL (Pan et al., 2019). A higher PBLH/ $PM_{2.5}$ means a stronger impact of $PM_{2.5}$ on the PBLH. Mean PBLH/ $PM_{2.5}$ values in spring, summer, autumn, and winter in Nanjing are 29.6, 38.8, 30.5, and 24.5, respectively, while in Beijing, they are 12.5, 20.4, 14.1, and 14.5, respectively. This suggests that summertime $PM_{2.5}$ has the greatest influence on the evolution of the PBL at the two sites. Also, the PBLH/ $PM_{2.5}$ ratio in Nanjing is always higher than that in Beijing, indicating that the PBLH is more sensitive to the variation in $PM_{2.5}$ mass concentration in Nanjing.

3.3. Differentiating the impact of scattering and absorbing aerosols on the PBLH

For differentiating the impact of scattering and absorbing aerosols on the PBLH, the mass ratio of scattering aerosols to BC (rBC) is calculated to represent the relative content of the two types of aerosols: $r\text{BC} = \frac{\text{Scattering aerosol}}{\text{Absorbing aerosol}}$. If the PBLH is positively correlated with rBC, this means that scattering aerosols have a stronger influence on the PBLH, while a negative correlation means that absorbing aerosols have a stronger influence on the PBLH.

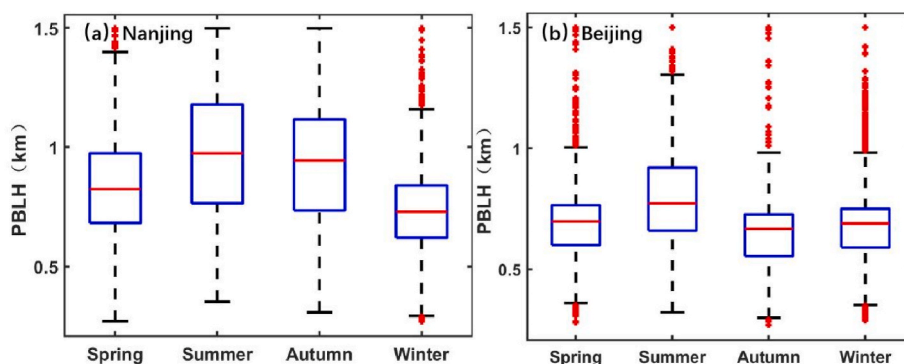


Fig. 2. Box plots of seasonal PBLH in (a) Nanjing and (b) Beijing. Boxes show the 25th, 50th, and 75th percentiles. Extremities show the 5th and 95th percentiles. Outliers are represented by red dots.

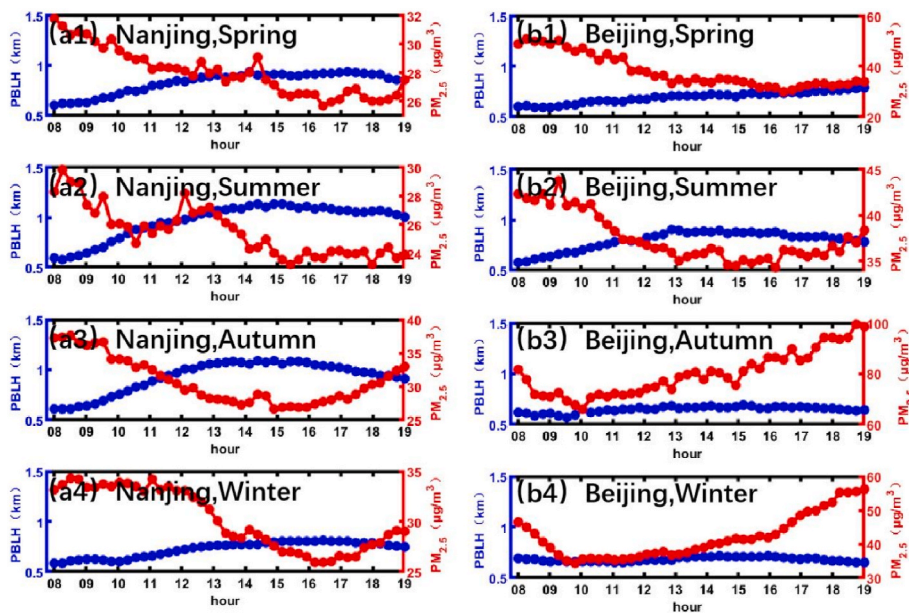


Fig. 3. Daytime variations of PBLH (blue lines) and $PM_{2.5}$ mass concentration (red lines) in spring, summer, autumn, and winter in (a1-a4) Nanjing and (b1-b4) Beijing.

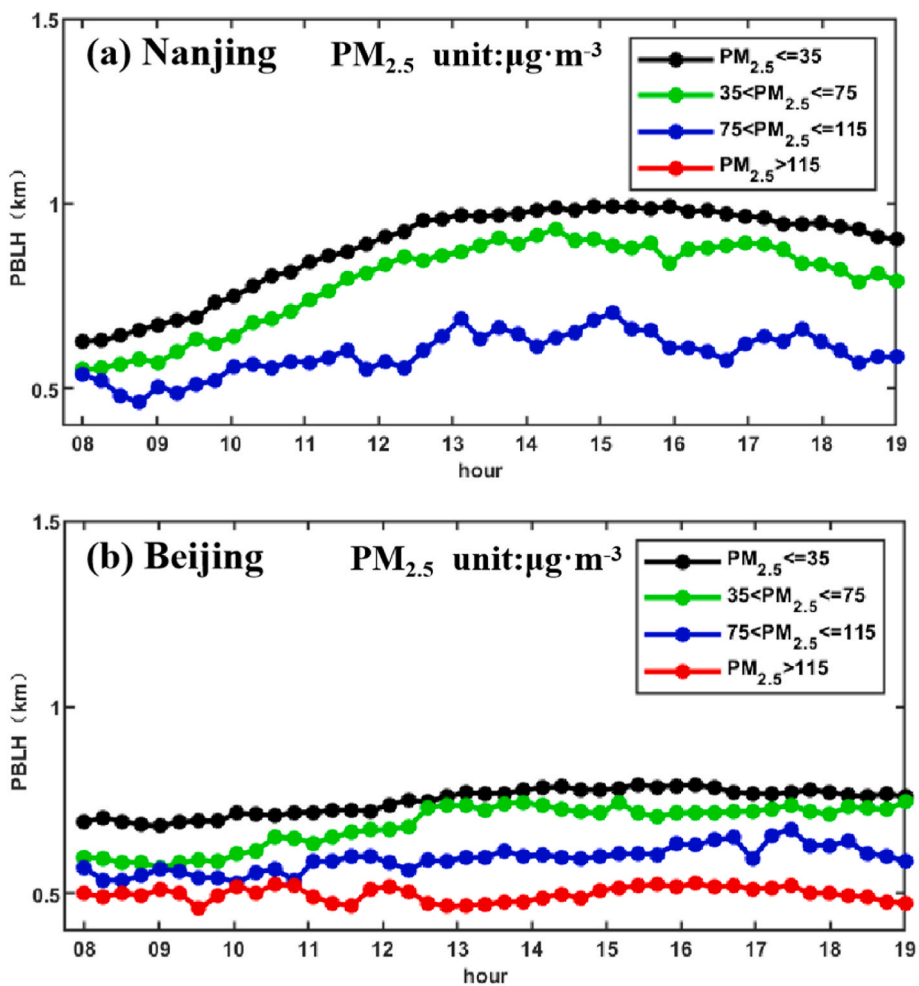


Fig. 4. Daytime variations of the PBLH at four pollution levels in (a) Nanjing and (b) Beijing. The heavily polluted level ($PM_{2.5} > 115 \mu g/m^3$) in Nanjing is missing because there were no heavily polluted days during the measurement period.

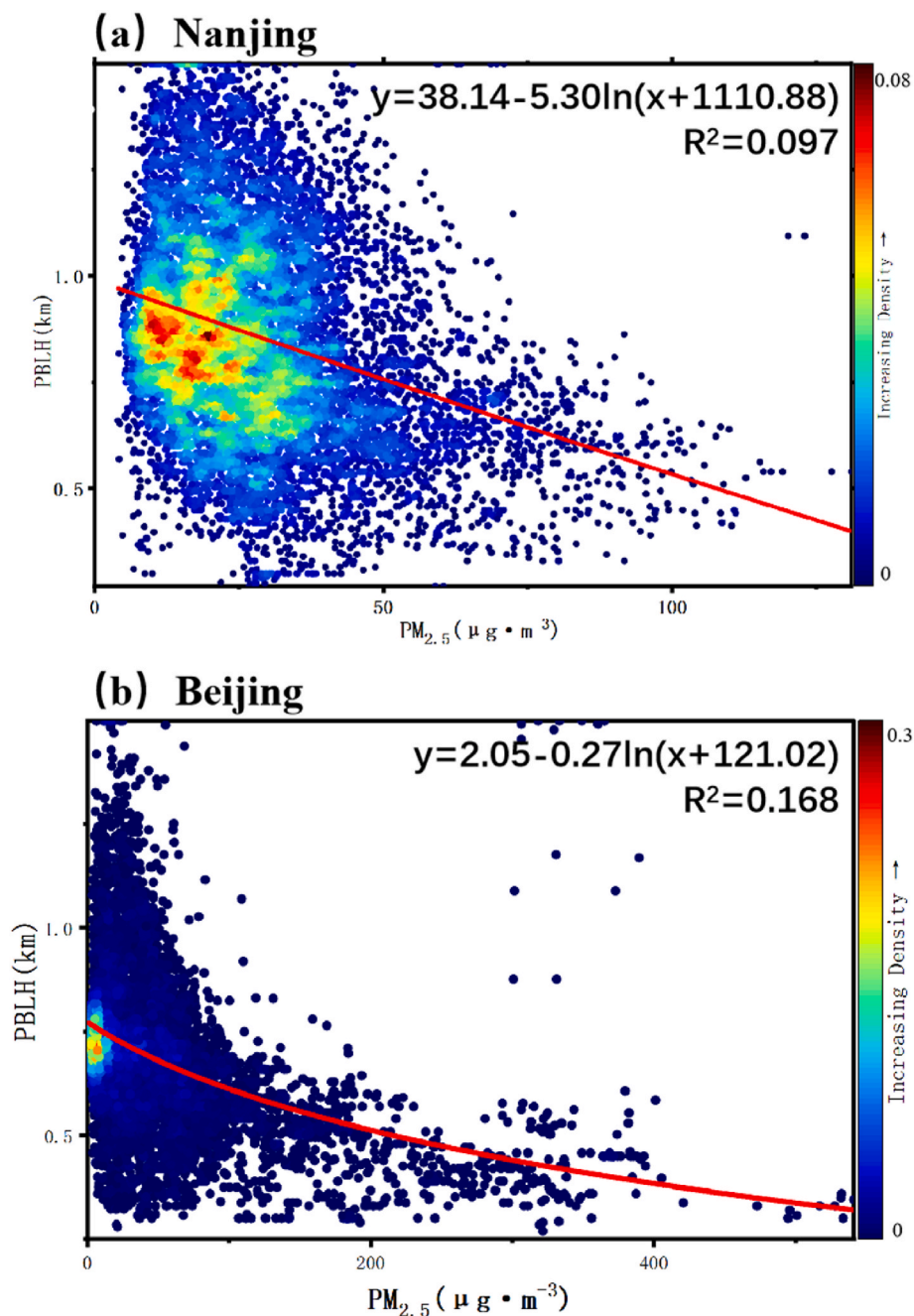


Fig. 5. Density diagrams of the relationship between PBLH and $PM_{2.5}$ mass concentration in (a) Nanjing and (b) Beijing. The color of the dot represents the probability, and red curves are fitted curves through the data. Logarithmic relations and coefficients of determination are given in each panel.

Fig. 6a shows a positive correlation between PBLH and rBC in Nanjing ($R = 0.13$). This suggests that the evolution of the PBLH in Nanjing is weakly affected by the difference in aerosol type. The scatter in Fig. 6b is concentrated, showing a clear negative correlation between PBLH and rBC in Beijing ($R = -0.18$). This indicates that absorbing aerosols play an important role in the evolution of the PBL at that location. Lee et al. (2007) reported that the aerosol single-scattering albedo is generally lower in Beijing than in Nanjing. Considering that both absorbing and scattering aerosols can inhibit the evolution of the PBL, results presented here suggest that aerosol type makes a difference in aerosol-PBL interactions in the two regions considered.

4. Summary and conclusions

The planetary boundary layer (PBL), the atmospheric layer closest to the Earth's surface, is a key region where various systems of the Earth interact. Exploring the factors influencing the evolution of the PBL based on field observations is important to constrain the effect of the PBL in many models. This study first compares aerosol-PBL interactions in two megacity stations (Beijing and Nanjing).

PBL heights (PBLHs) retrieved by the micro-pulse lidar suggest that monthly PBLH trends in Nanjing and Beijing were similar. PBLHs in summer and autumn were higher than in winter and spring, reaching maximum values in July. The average PBLH in Nanjing was about 200 m higher than in Beijing. In addition, $PM_{2.5}$ mass concentrations in Beijing were always higher than in Nanjing. There was an opposite monthly

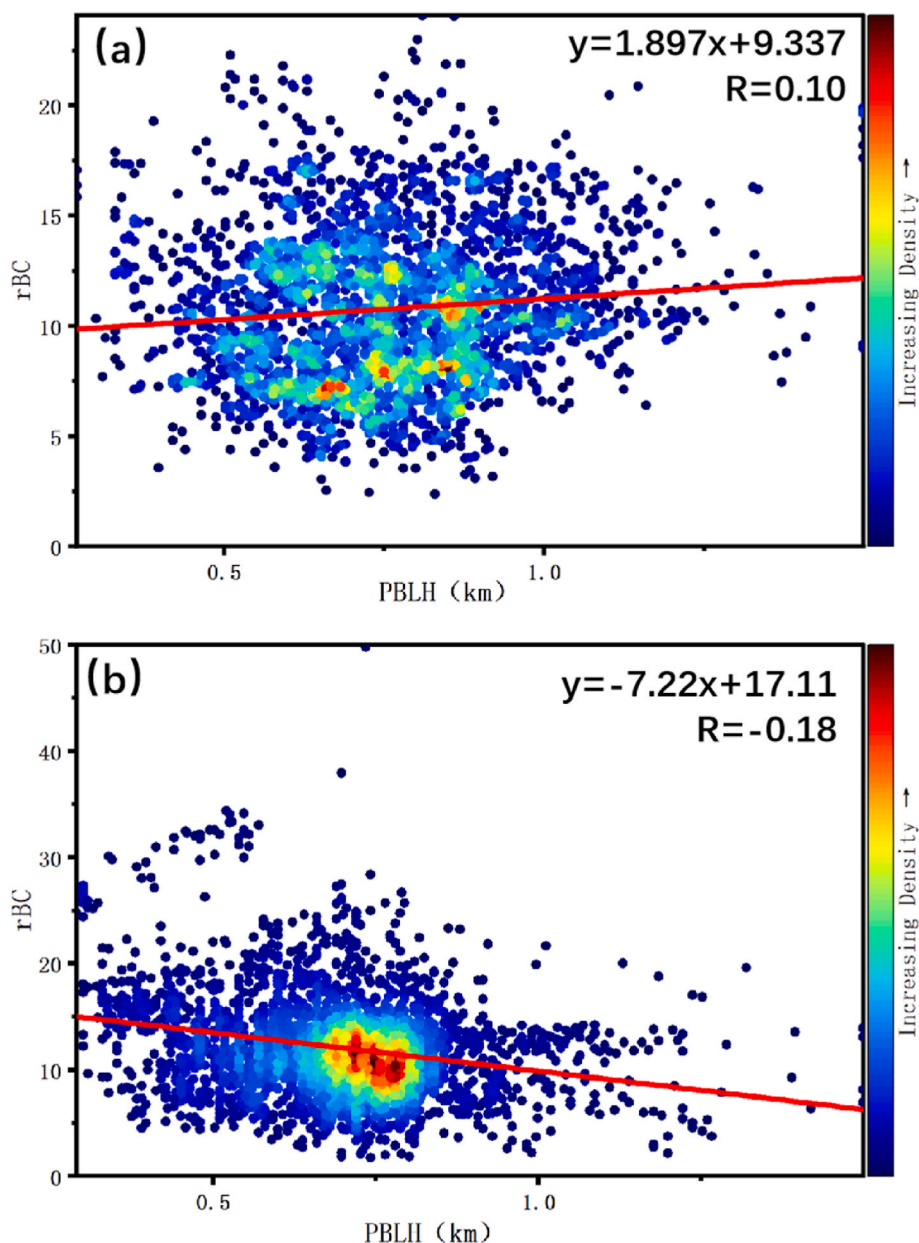


Fig. 6. Density diagrams of the relationship between rBC and PBLH in (a) Nanjing and (b) Beijing. The color of the dot represents the probability, and red lines are fitted lines through the data. Linear relations and correlation coefficients are given in each panel.

variation between PBLH and $PM_{2.5}$ mass concentration, which was more clearly seen in Nanjing in general, the PBLH and its variability were highest in summer. This is likely related to the high temperature and various synoptic patterns present in summer.

Overall, the PBLH clearly varied during the day in different seasons in Nanjing and Beijing. However, daytime variations of the PBLH in autumn and winter in Beijing were relatively small due to higher aerosol pollution levels. PBLHs under different aerosol pollution conditions were also compared. The PBLH decreased significantly as the $PM_{2.5}$ mass concentration increased, as did its daytime variation. There was a negative correlation between PBLH and $PM_{2.5}$ mass concentration, although the correlation coefficient was low. Compared with Nanjing, the correlation between PBLH and $PM_{2.5}$ mass concentration was stronger in Beijing. All this suggests the impact of aerosols on the evolution of the PBL.

The ratio of PBLH to $PM_{2.5}$ mass concentration indicates that summertime $PM_{2.5}$ had the greatest correlation on the evolution of the PBL

in all seasons. The PBLH in Nanjing was more sensitive to $PM_{2.5}$ mass concentration variations than in Beijing. Further results suggest that the evolution of the PBLH in Nanjing was weakly affected by the difference in aerosol type. Absorbing aerosols played an important role in the evolution of the PBL in Beijing. Our results highlight the regional difference in aerosol-PBL interactions due to aerosol type, a topic needing more research in the future.

Authorship contributions

XH and YYW led this work and prepared this paper; ZL designed the experiment and helped improving the quality of this paper; YS, XS, RZ, and YXW participated in the taken of field campaigns and processed the measurement data. All co-authors participated the discussion and figure processing in this paper.

Declaration of competing interest

The authors declare that they have no known competing financial interests or personal relationships that could have appeared to influence the work reported in this paper.

Data availability

Data will be made available on request.

Acknowledgements

This work was funded by the National Natural Science Foundation of China (NSFC) research project (grant no. 42030606, 42005067, and 92044303). We also thank all participants in the field campaigns for their tireless work and cooperation. Data will be made available on request.

Appendix A. Supplementary data

Supplementary data to this article can be found online at <https://doi.org/10.1016/j.atmosenv.2023.119861>.

References

- Beyrich, F., 1997. Mixing height estimation from sodar data — a critical discussion. *Atmos. Environ.* 31 (23), 3941–3953. [https://doi.org/10.1016/S1352-2310\(97\)00231-8](https://doi.org/10.1016/S1352-2310(97)00231-8).
- Blay-Carreras, E., Pino, D., Arellano, V., Boer, A., Coster, O., Hartogensis, O., Lohou, F., Lathon, M., Pietersen, H., 2014. Role of the residual layer and large-scale subsidence on the development and evolution of the convective boundary layer. *Atmos. Chem. Phys.* 14 (9), 4515–4530. <https://doi.org/10.5194/acp-14-4515-2014>.
- Boers, R., Eloranta, E., 1986. Lidar measurements of the atmospheric entrainment zone and the potential temperature jump across the top of the mixed layer. *Boundary-Layer Meteorol.* 34 (4), 357–375. <https://doi.org/10.1007/BF00120988>.
- Campbell, J.R., Dennis, L., Welton, E.J., Flynn, C.J., Turner, D.D., Spinhirne, J.D., Scott III, V.S., Hwang, I.H., 2002. Full-time, eye-safe cloud and aerosol lidar observation at atmospheric radiation measurement program sites: instruments and data processing. *J. Atmos. Ocean. Technol.* 19 (4), 431–441. [https://doi.org/10.1175/1520-0426\(2002\)019<0431:FTESCA>2.0.CO;2](https://doi.org/10.1175/1520-0426(2002)019<0431:FTESCA>2.0.CO;2).
- Campbell, J.R., Reid, J.S., Westphal, D.L., Zhang, J., Tackett, J.L., Chew, B.N., Welton, E. J., Shimizu, A., Sugimoto, N., Aoki, K., Winker, D.M., 2003. Characterizing the vertical profile of aerosol particle extinction and linear depolarization over Southeast Asia and the Maritime Continent: the 2007–2009 view from CALIOP. *Atmos. Res.* 122, 520–543. <https://doi.org/10.1016/j.atmosres.2012.05.007>.
- Collier, C.G., Davies, F., Bozier, K.E., Holt, A.R., Middleton, D.R., Pearson, G.N., Siemen, S., Willetts, D.V., Upton, G.J.G., Young, R.I., 2005. Dual-Doppler lidar measurements for improving dispersion models. *Bull. Am. Meteorol. Soc.* 86 (6), 825–838. <https://doi.org/10.1175/BAMS-86-6-825>.
- Deng, J.J., Wang, T.J., Liu, L., Jiang, F., 2010. Modeling heterogeneous chemical processes on aerosol surface. *Particuology* 8 (4), 308–318. <https://doi.org/10.1016/j.partic.2009.12.003>.
- Ding, A.J., Huang, X., Nie, W., Sun, J.N., Kerminen, V.M., Petäjä, T., Su, H., Cheng, Y.F., Yang, X.Q., Wang, M.H., Chi, X.G., Wang, J.P., Virkkula, A., Guo, W.D., Yuan, J., Wang, S.Y., Zhang, R.J., Wu, Y.F., Song, Y., Zhu, T., Zilitinkevich, S., Kulmala, M., Fu, C.B., 2016. Enhanced haze pollution by black carbon in megacities in China. *Geophys. Res. Lett.* 43, 2873–2879. <https://doi.org/10.1002/2016GL067745>.
- Forkel, R., Werhahn, J., Hansen, A.B., McKeen, S., Peckham, S., Grell, G., Suppan, P., 2011. Effect of aerosol-radiation feedback on regional air quality – a case study with WRF/Chem. *Atmos. Environ.* 53, 202–211. <https://doi.org/10.1016/j.atmosenv.2011.10.009>.
- Freire, L.S., Dias, N.L., 2013. Residual layer effects on the modeling of convective boundary layer growth rates with a slab model using FIFE data. *J. Geophys. Res.* Atmos. 118 (23), 12,869–12,878. <https://doi.org/10.1002/jgrd.50796>.
- Garratt, J.R., 1994. Review: the atmospheric boundary layer. *Earth Sci. Rev.* 37 (1–2), 89–134. [https://doi.org/10.1016/0012-8252\(94\)90026-4](https://doi.org/10.1016/0012-8252(94)90026-4).
- Guinot, B., Roger, J.C., Cachier, H., Wang, P., Bai, J., Yu, T., 2006. Impact of vertical atmospheric structure on Beijing aerosol distribution. *Atmos. Environ.* 40 (27), 5167–5180. <https://doi.org/10.1016/j.atmosenv.2006.03.051>.
- He, Q., Mao, J., Chen, J., Hu, Y., 2006. Observational and modeling studies of urban atmospheric boundary-layer height and its evolution mechanisms. *Atmos. Environ.* 40 (6), 1064–1077. <https://doi.org/10.1016/j.atmosenv.2005.11.016>.
- Hong, S.Y., Pan, H.L., 1996. Nonlocal boundary layer vertical diffusion in a medium-range forecast model. *Mon. Weather Rev.* 124 (10), 2322–2339. [https://doi.org/10.1175/1520-0493\(1996\)124<2322:NBLVDI>2.0.CO;2](https://doi.org/10.1175/1520-0493(1996)124<2322:NBLVDI>2.0.CO;2).
- Jacobson, M.Z., Kaufman, Y.J., 2006. Wind reduction by aerosol particles. *Geophys. Res. Lett.* 33 (24), L24814. <https://doi.org/10.1029/2006GL027838>.
- Jacobson, M.Z., Kaufman, Y.J., Rudich, Y., 2007. Examining feedbacks of aerosols to urban climate with a model that treats 3-D clouds with aerosol inclusions. *J. Geophys. Res. Atmos.* 112, D24205. <https://doi.org/10.1029/2007JD008922>.
- Kan, H., London, S.J., Chen, G., Zhang, Y., Song, G., Zhao, N., Jiang, L., Chen, B., 2008. Season, sex, age, and education as modifiers of the effects of outdoor air pollution on daily mortality in Shanghai, China: the public health and air pollution in Asia (PAPA) study. *Environ. Health Perspect.* 116 (9), 1183–1188. <https://doi.org/10.1289/ehp.10851>.
- Lee, K.H., Li, Z., Wong, M.S., Xin, J., Hao, W.M., Zhao, F., 2007. Aerosol single scattering albedo estimated across China from a combination of ground and satellite measurements. *J. Geophys. Res. Atmos.* 112 (D22S15). <https://doi.org/10.1029/2007JD009077>.
- Li, Z., Lau, W.K.M., Ramanathan, V., Wu, G., Ding, Y., Manoj, M.G., Liu, J., Qian, Y., Li, J., Zhou, T., Fan, J., Rosenfeld, D., Ming, Y., Wang, Y., Huang, J., Wang, B., Xu, X., Lee, S.-S., Cribb, M., Zhang, F., Yang, X., Zhao, C., Takemura, T., Wang, K., Xia, X., Yin, Y., Zhang, H., Guo, J., Zhai, P.M., Sugimoto, N., Babu, S.S., Brasseur, G. P., 2016. Aerosol and monsoon climate interactions over Asia. *Rev. Geophys.* 54 (4), 866–929. <https://doi.org/10.1002/2015RG000500>.
- Li, Z., Guo, J., Ding, A., Liao, H., Liu, J., Sun, Y., Wang, T., Xue, Zhang, H., Zhu, B., 2017. Aerosol and boundary-layer interactions and impact on air quality. *Natl. Sci. Rev.* 4 (6), 810–833. <https://doi.org/10.1093/nsr/nwx117>.
- Liu, Q., Wang, Y., Kuang, Z., Fang, S., Chen, Y., Kang, Y., Zhang, H., Wang, D., Fu, Y., 2016. Vertical distributions of aerosol optical properties during haze and floating dust weather in Shanghai. *Journal of Meteorological Research* 30 (4), 598–613. <https://doi.org/10.1007/s13351-016-5092-4>.
- Lou, M., Guo, J., Wang, L., Xu, H., Chen, D., Miao, Y., Lv, Y., Li, Y., Guo, X., Ma, S., Li, J., 2019. On the relationship between aerosol and boundary layer height in summer in China under different thermodynamic conditions. *Earth Space Sci.* 6 (5), 887–901. <https://doi.org/10.1029/2019EA000620>.
- Miao, Y., Guo, J., Liu, S., Liu, H., Li, Z., Zhang, W., Zhai, P., 2017. Classification of summertime synoptic patterns in Beijing and their associations with boundary layer structure affecting aerosol pollution. *Atmos. Chem. Phys.* 17 (4), 3097–3110. <https://doi.org/10.5194/acp-17-3097-2017>.
- Pan, L., Xu, J., Tie, X., Mao, X., Gao, W., Chang, L., 2019. Long-term measurements of planetary boundary layer height and interactions with PM_{2.5} in Shanghai, China. *Atmos. Pollut. Res.* 10 (3), 989–996. <https://doi.org/10.1016/j.apr.2019.01.007>.
- Pandithurai, G., Seethala, C., Murthy, B.S., Devara, P.C.S., 2008. Investigation of atmospheric boundary layer characteristics for different aerosol absorptions: case studies using CAPS model. *Atmos. Environ.* 42 (19), 4755–4768. <https://doi.org/10.1016/j.atmosenv.2008.01.038>.
- Park, S.S., Jung, Y., Lee, Y.G., 2016. Spectral dependence on the correction factor of erythemal UV for cloud, aerosol, total ozone, and surface properties: a modeling study. *Adv. Atmos. Sci.* 33 (7), 865–874. <https://doi.org/10.1007/s00376-016-5201-4>.
- Peck, J., Gonzalez, L.A., Williams, L.R., Xu, W., Croteau, P.L., Timko, M.T., Jayne, J.T., Worsnop, D.R., Miake-Lye, R.C., Smith, K.A., 2016. Development of an aerosol mass spectrometer lens system for PM_{2.5}. *Aerosol. Sci. Technol.* 50, 781–789. <https://doi.org/10.1080/02786826.2016.1190444>.
- Péré, J.C., Mallet, M., Pont, V., Bessagnet, B., 2011. Impact of aerosol direct radiative forcing on the radiative budget, surface heat fluxes, and atmospheric dynamics during the heat wave of summer 2003 over western Europe: a modeling study. *J. Geophys. Res. Atmos.* 116, D23119. <https://doi.org/10.1029/2011jd016240>.
- Qu, Y., Han, Y., Wu, Y., Gao, P., Wang, T., 2017. Study of PBLH and its correlation with particulate matter from one-year observation over Nanjing, Southeast China. *Rem. Sens.* 9 (7), 668. <https://doi.org/10.3390/rs9070668>.
- Reen, B.P., Stauffer, D.R., Davis, K.J., 2014. Land-surface heterogeneity effects in the planetary boundary layer. *Boundary-Layer Meteorol.* 150 (1), 1–31. <https://doi.org/10.1007/s10546-013-9860-8>.
- Song, L., Deng, T., Li, Z., Wu, C., He, G., Li, F., Wu, M., Wu, D., 2021. Retrieval of boundary layer height and its influence on PM_{2.5} concentration based on lidar observation over Guangzhou. *J. Trop. Meteorol.* 27 (3), 303–318. <https://doi.org/10.46267/j.1006-8775.2021.027>.
- Stull, R.B., 1988. *An Introduction to Boundary Layer Meteorology*. Springer, Netherlands, Dordrecht. <https://doi.org/10.1007/978-94-009-3027-8>.
- Su, T., Li, Z., Li, C., Li, J., Han, W., Shen, C., Tan, W., Wei, J.M., Guo, J., 2020. The significant impact of aerosol vertical structure on lower atmosphere stability and its critical role in aerosol–planetary boundary layer (PBL) interactions. *Atmos. Chem. Phys.* 20 (6), 3713–3724. <https://doi.org/10.5194/acp-20-3713-2020>.
- Therry, G., Lacarrère, P., 1983. Improving the eddy kinetic energy model for planetary boundary layer description. *Boundary-Layer Meteorol.* 25 (1), 63–88. <https://doi.org/10.1007/bf00122098>.
- Tie, X., Madronich, S., Li, G., Ying, Z., Zhang, R., Garcia, A., Taylor, J., Liu, Y., 2007. Characterizations of chemical oxidants in Mexico City: a regional chemical/dynamical model (WRF-Chem) study. *Atmos. Environ.* 41 (9), 1989–2008. <https://doi.org/10.1016/j.atmosenv.2006.10.053>.
- Wang, Y., Li, Z., Wang, Q., Jin, X., Yan, P., Cribb, M., Li, Y., Yuan, C., Wu, H., Wu, T., Ren, R., Cai, Z., 2021. Enhancement of secondary aerosol formation by reduced anthropogenic emissions during Spring Festival 2019 and enlightenment for regional PM_{2.5} control in Beijing. *Atmos. Chem. Phys.* 21 (2), 915–926. <https://doi.org/10.5194/acp-21-915-2021>.
- Wei, W., Zhang, H.S., Schmitt, F.G., Huang, Y.X., Cai, X.H., Song, Y., Huang, X., Zhang, H., 2017. Investigation of turbulence behaviour in the stable boundary layer using arbitrary-order Hilbert spectra. *Boundary-Layer Meteorol.* 163 (2), 311–326. <https://doi.org/10.1007/s10546-016-0227-9>.
- Wendisch, M., Hellmuth, O., Ansmann, A., Heintzenberg, J., Engelmann, R., Althausen, D., Eichler, H., Müller, D., Hu, M., Zhang, Y., Mao, J., 2008. Radiative

- and dynamic effects of absorbing aerosol particles over the Pearl River Delta, China. *Atmos. Environ.* 42 (25), 6405–6416. <https://doi.org/10.1016/j.atmosenv.2008.02.033>.
- Xu, W., Croteau, P., Williams, L., Canagaratna, M., Onasch, T., Cross, E., Zhang, X., Robinson, W., Worsnop, D., Jayne, J., 2017. Laboratory characterization of an aerosol chemical speciation monitor with PM_{2.5} measurement capability. *Aerosol. Sci. Technol.* 51, 69–83. <https://doi.org/10.1080/02786826.2016.1241859>.
- Yu, H., Liu, S.C., Dickinson, R.E., 2002. Radiative effects of aerosols on the evolution of the atmospheric boundary layer. *J. Geophys. Res. Atmos.* 107, 4142. <https://doi.org/10.1029/2001JD000754>.
- Zhang, Y., Wen, X.Y., Jang, C.J., 2010. Simulating chemistry-aerosol-cloud-radiation-climate feedbacks over the continental U.S. using the online-coupled Weather Research Forecasting Model with chemistry (WRF/Chem). *Atmos. Environ.* 44 (29), 3568–3582. <https://doi.org/10.1016/j.atmosenv.2010.05.056>.
- Zhang, Y., Tang, L., Croteau, P.L., Favez, O., Sun, Y., Canagaratna, M.R., Wang, Z., Couvidat, F., Albinet, A., Zhang, H., Sciare, J., Prévôt, A.S.H., Jayne, J.T., Worsnop, D.R., 2017. Field characterization of the PM_{2.5} aerosol chemical speciation monitor: insights into the composition, sources, and processes of fine particles in eastern China. *Atmos. Chem. Phys.* 17, 14,501–14,517. <https://doi.org/10.5194/acp-17-14501-2017>.